Optimal Contact Force Distribution for Multi-Limbed Robots

Dennis W. Hong[1]
Professor
Mechanical Engineering Department,
Virginia Tech,
Blacksburg, VA 24061
e-mail: dhong@vt.edu

Raymond J. Cipra
School of Mechanical Engineering,
Purdue University,
585 Purdue Mall,
West Lafayette, IN 47907-2088
e-mail: cipra@ecn.purdue.edu

One of the inherent problems of multi-limbed mobile robotic systems is the problem of multi-contact force distribution; the contact forces and moments at the feet required to support it and those required by its tasks are indeterminate. A new strategy for choosing an optimal solution for the contact force distribution of multi-limbed robots with three feet in contact with the environment in three-dimensional space is presented. The incremental strategy of opening up the friction cones is aided by using the "force space graph" which indicates where the solution is positioned in the solution space to give insight into the quality of the chosen solution and to provide robustness against disturbances. The "margin against slip with contact point priority" approach is also presented which finds an optimal solution with different priorities given to each foot contact point. Examples are presented to illustrate certain aspects of the method and ideas for other optimization criteria are discussed. [DOI: 10.1115/1.2179462]

Keywords: multi-contact force distribution, contact force solution, optimization, margin against slip, contact point priority, force space graph, solution volume representation, multi-limbed robots

1 Introduction

This paper presents a strategy for choosing the optimal force distribution solution in the given solution space (description of all the possible solutions) as the second step in finding the optimal set of foot contact forces for a multi-limbed mobile robotic system in contact with its environment with three feet contact. Since the limbs of the robot have enough joints and are actively controlled, the contact forces at the feet need to be explicitly chosen to ensure that the robot does not lose its balance and does not slip at the foot. One of the major difficulties associated with finding the force distribution solution has been the indeterminate nature of the problem. Any system with three or more contact points makes it an underspecified system involving redundancy since there are more unknowns than the number of equations. The other major difficulty associated with the problem of multi-contact force distribution has been the nonlinear nature of the three-dimensional friction cone model.

2 Background and Previous Work

2.1 Multi-Contact Force Distribution Problem. For a multi-limbed robot to maintain a stable position on a steep incline or on rough terrain, there are two key issues that need to be considered: one is losing balance due to external forces such as gravity, and the other is the slipping between the feet and the surface. In other words, all the forces acting on the robot including the foot contact forces should satisfy the static equilibrium equations while, at the same time, each foot contact force should be in the friction cone at their contact point to avoid slipping. Thus, the force distribution problem is a statically indeterminate problem formulated by a set of equality constraints (static force moment equilibrium equations) and a set of nonlinear inequality constraints (friction constraints). The goal is to find the solution that satisfies these constraints and maximizes the objectives given

by the optimization criteria.

Most previous work in this area proposed using pseudo inverse [1,2] and/or various optimization techniques for finding a solution for a problem formulated as a constrained, optimization problem using specific objective functions [3–11]. The problem is then solved by linearizing the friction cone constraints first and then applying various linear programming techniques. These approaches were also used for multi-fingered robotic hand grasping [8,12,13] and multiple robot manipulators working together. However, these methods were often too slow for real time computation and were limited in many ways. There were also attempts to find a suboptimal solution more quickly to make it fast enough for real time computation [13,14].

2.2 Two-Step Method. Unlike other methods previously developed where a single solution to a constrained optimization problem is immediately found from maximizing an objective function(s) under constraints, Hong and Cipra [15–17] introduced a two-step approach in solving the multi-contact force distribution problem. First, the entire solution space that satisfies all constraints is found (finding the solution space), and then a solution in that space which will give the best results for the objectives given by the chosen optimization criteria is chosen as its optimal solution (choosing the optimal solution). Finding the description of the entire solution space first provides an intuitive visual map of how well the solution space is formed for the given conditions of the system. This is very important and can be useful for the higher-level motion planner for deciding on potential foot placement locations on the surface or for choosing the internal configuration of the robot (posture) when moving. Choosing a solution in the solution space next will let us see in advance where this solution is positioned in the solution space to give insight into the quality of that chosen solution and to provide a measure of robustness against disturbances, thus will allow us to choose the "best" solution for the situation.

In [15], the method developed was applicable only to a climbing tethered mobile robot with a single cable and two feet contact. In this paper we present a more general method for choosing the optimal contact force solution in its solution space for multi-limbed mobile robots with three feet contact as the second step in

---

Copyright © 2006 by ASME

finding the optimal contact force distribution solution. The methods for both cases are similar in concept, but the method presented in this paper for the three feet contact case is more general and thus can also be used for finding the optimal force distribution for the one cable-two feet contact case as well. The first step of finding the solution space was presented in Hong and Cipra [16–18].

2.3 Finding the Solution Space. As the first step in finding the optimal contact force distribution, Hong and Cipra [16–18] presented a new analytical method for determining, describing, and visualizing the solution space for the contact force distribution of multi-limbed robots with three feet in contact with the environment in three-dimensional space. The "point contact with friction" model [19] is used where only a normal force and a tangential force are acting on the contact point (as opposed to the "soft finger contact" model [20] where the contact point is also subjected to a moment about the normal.) The foot contact forces are first resolved into strategically defined foot contact force components to decouple them for simplifying the solution process, and then the static equilibrium equations are applied to find certain contact force components and the relationship between the others. Using the friction cone equation at each foot contact point and the known contact force components, the problem is transformed into a geometrical one to find the ranges of contact forces and the relationship between them that satisfy the friction constraint. Using geometric properties of the friction cones and by simple manipulation of their conic sections, the entire solution space which satisfies the static equilibrium and friction constraints at each contact point can be found. Two representation schemes, the "force space graph" and the "solution volume representation," are developed for describing and visualizing the solution space which gives an intuitive visual map of how well the solution space is formed for the given conditions of the system. Once the description of the entire solution space is found, a solution can be chosen in this solution space next which maximizes the objectives given by the chosen optimization criteria.

3 Example System and its Solution Space

3.1 Mobile Robotic System. The multi-limbed mobile robotic system under consideration is assumed to move in a quasi-static manner, by stably supporting itself against the environment surfaces using its three feet, moving a free limb to a new position and setting it down while lifting a foot that was in contact with the surface, and then slowly changing its internal configuration to a new posture. The 'three feet contact' implies that there are only three feet in contact with the surface at a given time, and thus does not mean that the robot only has three feet.

To illustrate the method, a robotic system with three feet in contact with the surface will be used as an example. The parameters used to define this example system and the numbers presented here as results could assume any units as long as they have the correct dimensions corresponding to its type (force or length). Position vectors for the three foot contact points C_1, C_2, and C_3 expressed in, and from the origin of the body coordinate frame are given as

$$\bar{r}_{C1} = \{4.0, 4.0, -3.9\}$$

$$\bar{r}_{C2} = \{-4.0, 4.1, -4.0\}$$

$$\bar{r}_{C3} = \{0.0, -4.0, -4.1\} \tag{1}$$

and at each foot contact point C_1, C_2, and C_3, the foot contact coordinate frames are set following the rules defined (Hong and Cipra [16–18]) using the four unit contact force component vectors e_α, e_β, e_γ and e_δ. The unit surface normal direction vectors u_{N1}, u_{N2} and u_{N3} are given as

$$\bar{u}_{N1} = \{-0.577, -0.577, 0.577\}$$
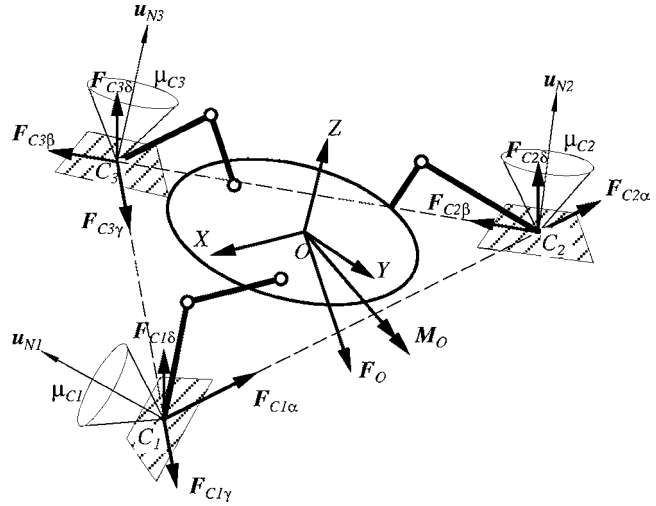
Fig. 1 The force system

$$\bar{u}_{N2} = \{0.667, -0.333, 0.667\}$$

$$\bar{u}_{N3} = \{0.000, 0.707, 0.707\} \tag{2}$$

and their corresponding friction coefficients μ_{C1}, μ_{C2} and μ_{C3} are

$$\mu_{C1} = 0.2, \quad \mu_{C2} = 0.32, \quad \mu_{C3} = 0.15 \tag{3}$$

The known external force F_O and the known external moment M_O expressed in the body coordinate frame and acting on the origin O are

$$\bar{F}_O = \{0.0, 0.1, -8.0\}, \quad \bar{M}_O = \{2.0, 0.1, 0.0\} \tag{4}$$

This example system is represented in Fig. 1 with the friction cones shown at each contact point.

3.2 Solution Space and Force Space Graph. As the first step, the solution space and its force space graph must be found using the strategy introduced in Hong and Cipra [16–18]. Among the nine unknown foot contact force components, three of them are explicitly found (the e_δ component forces $F_{C1\delta}$, $F_{C2\delta}$ and $F_{C3\delta}$) by summing the moments about e_α, e_β and e_γ unit force component vectors. For the example system these are found as

$$F_{C1\delta} = 1.901, \quad F_{C2\delta} = 1.876, \quad F_{C3\delta} = 4.223 \tag{5}$$

Another three components ($F_{C1\gamma}$, $F_{C2\alpha}$ and $F_{C3\beta}$) are given as linear relationships to the other three components ($F_{C1\alpha}$, $F_{C2\beta}$ and $F_{C3\gamma}$) by summing the forces in the e_δ direction at the three contact points as

$$F_{C1\gamma} = 0.088 - F_{C3\gamma} \tag{6}$$

$$F_{C2\alpha} = -0.048 - F_{C1\alpha} \tag{7}$$

$$F_{C3\beta} = 0.033 - F_{C2\beta} \tag{8}$$

Then, using the presented strategy, the last three components ($F_{C1\alpha}$, $F_{C2\beta}$ and $F_{C3\gamma}$) are described as possible ranges and constraints by reducing the problem into the following set of three quadratic inequality equations which describes the solution space of the example system

$$E_{C1}(F_{C3\gamma}, F_{C1\alpha}) = 0.397F_{C3\gamma}^2 + 0.671F_{C1\alpha}^2 - 0.019F_{C3\gamma}F_{C1\alpha}$$
$$- 1.863F_{C3\gamma} - 1.323F_{C1\alpha} + 2.443$$
$$\leq 0 \tag{9}$$
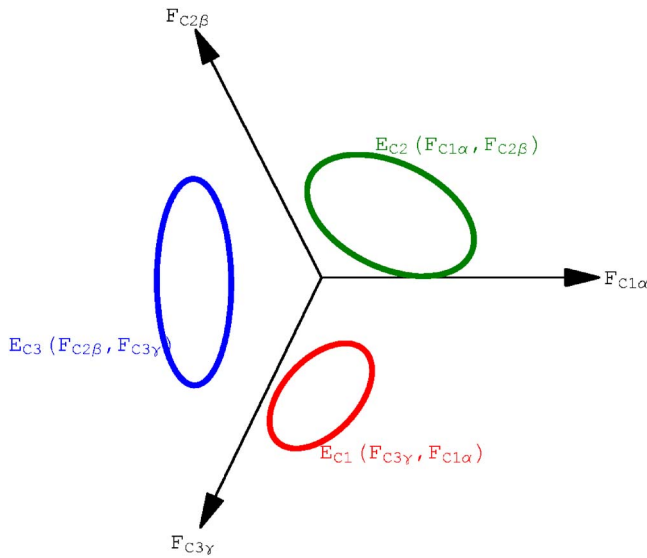
Fig. 2 The force space graph representation

$$E_{C2}(F_{C1\alpha}, F_{C2\beta}) = 0.492F_{C1\alpha}^2 + 0.621F_{C2\beta}^2 + 0.029F_{C1\alpha}F_{C2\beta}$$
$$- 1.818F_{C1\alpha} - 1.610F_{C2\beta} + 1.719$$
$$\leq 0 \qquad (10)$$

$$E_{C3}(F_{C2\beta}, F_{C3\gamma}) = 0.579F_{C2\beta}^2 + 0.571F_{C3\gamma}^2 + 0.357F_{C2\beta}F_{C3\gamma}$$
$$- 3.883F_{C2\beta} - 3.895F_{C3\gamma} + 9.184$$
$$\leq 0 \qquad (11)$$

Any set of forces ($F_{C1\alpha}$, $F_{C2\beta}$, and $F_{C3\gamma}$) that satisfy this set of three constraints (E_{C1}, E_{C2}, and E_{C3}) will satisfy all sets of static equilibrium and friction constraints, and thus is defined as the solution space. Figure 2 shows the force space graph representation [16–18] of the solution space described by this set of three constraints. This representation helps to visualize the three quadratic inequality constraints and the solution space that satisfies them, and will also be used as a tool for choosing a solution in the solution space.

Figure 3(a) shows an example of a set of three contact force components $F_{C1\alpha}$, $F_{C2\beta}$, and $F_{C3\gamma}$ on the force space graph as a valid solution where points P_1, P_2, and P_3 defined by these three contact force components are in each of their transformed conic sections, thus satisfying all constraints. Figure 3(b) shows an example of an invalid solution on the force space graph where point P_1 is not inside its transformed conic section $E_{C1}(F_{C3\gamma}, F_{C1\alpha})$ and thus will slip at contact point C_1.

Using the strategy presented in Hong and Cipra [16–18], we now have a representation of all the combinations of the foot
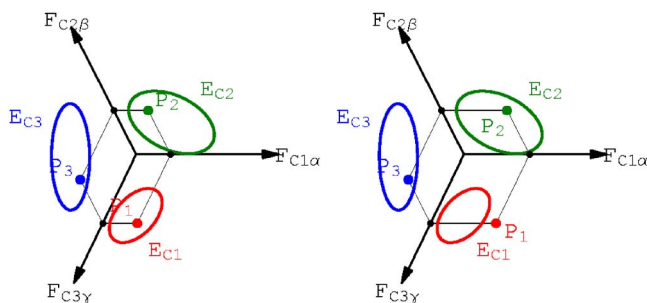
Fig. 3 Valid/invalid solution on the force space graph (a) a valid solution, (b) an invalid solution (slip at C_1)

contact force distributions possible that satisfy all static equilibrium and friction constraints as the entire solution space. Among the nine unknown force components, three of them ($F_{C1\delta}$, $F_{C2\delta}$, and $F_{C3\delta}$) are explicitly specified (Eq. (5)), another three components ($F_{C1\alpha}$, $F_{C2\beta}$ and $F_{C3\gamma}$) are given as possible ranges and constraints by three quadratic inequality equations (Eqs. (9)–(11)) represented by the force space graph, and the last three components ($F_{C1\gamma}$, $F_{C2\alpha}$, and $F_{C3\beta}$) are given as linear relationships to the other components (Eqs. (6)–(8)). Now choosing a solution set is a matter of specifying the three contact force component variables $F_{C1\alpha}$, $F_{C2\beta}$ and $F_{C3\gamma}$ that satisfy the three quadratic inequality equations (Eqs. (9)–(11)) represented by the force space graph, using the chosen criteria.

4 Choosing the Optimal Solution in the Solution Space

Once the description of the solution space which satisfies the force moment equilibrium equations and the friction constraints is found, any solution picked in the solution space will at least guarantee that the robot will be in static equilibrium without slipping. However, it is desirable to choose a solution in that solution space that best suits the objectives as the optimal solution.

For the three feet contact case, the overall strategy is similar to that for the "one cable-two feet contact case" [15]; however, the entire solution space which satisfies the static equilibrium and friction constraints at each contact point is described in terms of three parameters instead of one, and thus the strategy for choosing the optimal solution is more complex.

The force space graph representation of the solution space and its geometric properties will be used as a tool in choosing the optimal solution. We first introduce the concept of the margin against slip criterion and contact point priority and then demonstrate the method of choosing the optimal solution using the force space graph using the example system. A discussion of different possible optimization approaches is presented next.

4.1 Margin Against Slip Criterion With Contact Point Priority

4.1.1 Margin Against Slip Criterion. Among the many different possible optimization criteria, maximizing the margin against slipping is especially an interesting and potentially useful one since it can be used to quantify the quality of the chosen solution and describe the position of that solution in the solution space. Physically this value could indicate how far the chosen solution is from the nearest possible solution that will make a foot slip (boundary of the friction cone), thus can be used to represent a solution's robustness against disturbances and as a measure for choosing the optimal solution.

We define the margin against slip (N_{Ci}) as the ratio of the smallest angle between the chosen force solution vector and the friction cone ($\phi_{Ci} - \phi_{Ci}^*$), over the angle between the friction cone and its center axis (ϕ_{Ci}) where, for contact point C_i, these are defined by

$$\phi_{Ci} = \tan^{-1} \mu_{Ci} \qquad (12)$$

and

$$\phi_{Ci}^*(t) = \cos^{-1}\left[\frac{\bar{u}_{Ni} \cdot \bar{F}_{Ci}(t)}{\|\bar{u}_{Ni}\| \|\bar{F}_{Ci}(t)\|} \right] \qquad (13)$$

as shown in Fig. 4. Thus, for contact point C_i, the margin against slip (N_{Ci}) is represented by

$$N_{Ci}(t) = 1 - \frac{\phi_{Ci}^*(t)}{\phi_{Ci}} \qquad (14)$$

By definition, a margin against slip can only have a value between 0 and 1. A margin against slip of 1 indicates that the force solution vector coincides with the center axis of the friction cone or the surface normal vector ($\phi_{Ci}^* = 0$), thus the contact force at this case is pure normal force with no friction force components. A
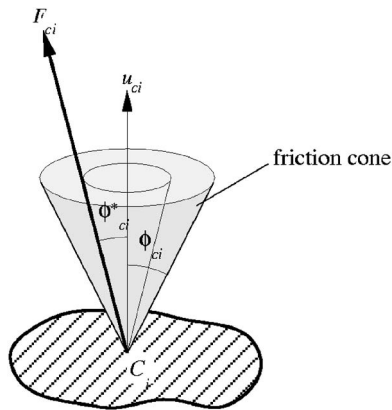
Fig. 4 Defining margin against slip

margin against slip of 0 indicates that the chosen force solution vector is at the boundary of the friction cone ($\phi_{Ci}^* = \phi_{Ci}$) and thus is at the verge of slipping. When there is a disturbance that causes any changes in the system, the higher the margin against slip the better because this would decrease the chances of slipping since this means that there is a larger "buffer zone" before the contact force acts outside its friction cone which will cause slipping.

However, unlike the method developed for the one cable-two feet contact case (Hong and Cipra [15]), we do not use the equation defining the margin against slip (Eq. (14)) directly to find the optimal solution, but rather use a different approach while applying the same concept to choose the optimal solution. Since the margin against slip for a contact point indicates how far the chosen solution is from the nearest possible solution that will make a foot slip (boundary of the friction cone), to maximize this factor is to find the contact force which is closest to its friction cone center axis (or the surface normal vector) while still satisfying all constraints. In other words, the set of contact forces that satisfy all constraints with the smallest friction coefficients (narrowest friction cones) at each contact point would be the optimal solution for the given system.

Using this idea, we apply an incremental strategy to find the set of contact forces as the optimal solution: starting from a value of zero for the friction coefficients for all three contact points, we check if a solution exists. If no solution exists, we increase the friction coefficients (open up the friction cones) by a specified amount for each contact point and check again if a solution exists.

This process is repeated until a solution is found, or until all three friction coefficients reach their actual values. The first solution found in this process would then be the optimal solution following the margin against slip criteria since ϕ_{Ci}^* would be the smallest implying that the margin against slip (N_{Ci}) is the largest. If no solution is found in the process, no solution exists for the given system.

4.1.2 Contact Point Priority. If the rate of opening up the friction cone ($\Delta\phi_{Ci}^*/\phi_{Ci}$) is the same for all three contact points, then the margin against slip (N_{Ci}) found using this strategy would be the same for all three contact points. However, this rate ($\Delta\phi_{Ci}^*/\phi_{Ci}$) of increasing the value of ϕ_{Ci}^* (the rate of opening up the friction cones) does not need to be the same for each contact point. Having different rates of friction coefficient increments between each contact point gives a particular foot contact point a higher priority over the others. This is similar to the contact point priority concept developed for the one cable-two feet contact case (Hong and Cipra [15]). An example would be when one foot placement point is more critical than the other's such as when it is near an edge of a cliff, and would like to make sure that it will not slip at that point and cause a catastrophic failure. The smaller the rate of increment of a friction coefficient (the slower the opening up of a friction cone), the higher the priority that contact point gets in finding the optimal solution, since the contact force found for that contact point would be closer to the center axis of its friction cone (or the surface normal vector) than the others if a solution does exist. This opening rate of the friction cone is based on both its assigned priority (P_{Ci}) and its actual friction coefficient value μ_{Ci} (thus, the value of ϕ_{Ci}). When opening each cone, the ratio of $\Delta\phi_{Ci}^*$ (the increment of the intermediate friction cone angle ϕ_{Ci}^*) to ϕ_{Ci} (the actual friction cone angle) between the three contact points C_1, C_2 and C_3 is based on

$$\frac{1}{P_{C1}}:\frac{1}{P_{C2}}:\frac{1}{P_{C3}} = \frac{\Delta\phi_{C1}^*}{\phi_{C1}}:\frac{\Delta\phi_{C2}^*}{\phi_{C2}}:\frac{\Delta\phi_{C3}^*}{\phi_{C3}} \tag{15}$$

where $P_{C1}:P_{C2}:P_{C3}$ is the priority ratio between the three contact points C_1, C_2 and C_3. Thus when finding the optimal solution, the "intermediate" friction cone is opened up from the center axis (μ_{Ci}^* value of zero) with a cone angle increment $\Delta\phi_{Ci}^*$ based on its assigned priority and actual friction cone angle ϕ_{Ci} as shown in Eq. (15), until a solution is found or until it reaches its actual friction cone (μ_{Ci}^* reaches the value of μ_{Ci}).

Figure 5 shows the process of opening up the friction cones on the force space graph for the example system. Figure 5(*a*) shows
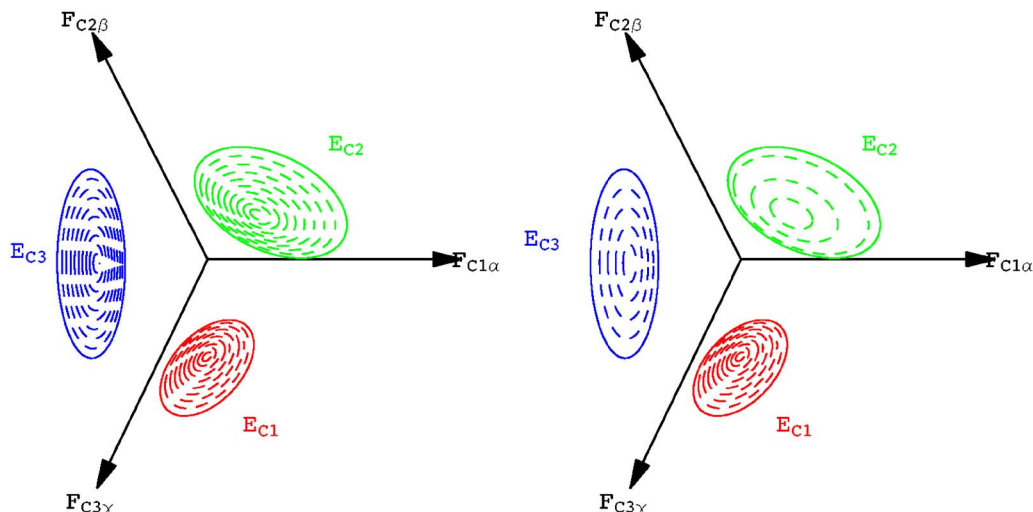
Fig. 5 Opening up the friction cones (a) $P_{C1}:P_{C2}:P_{C3}=1:1:1$, (b) $P_{C1}:P_{C2}:P_{C3}=3:1:2$
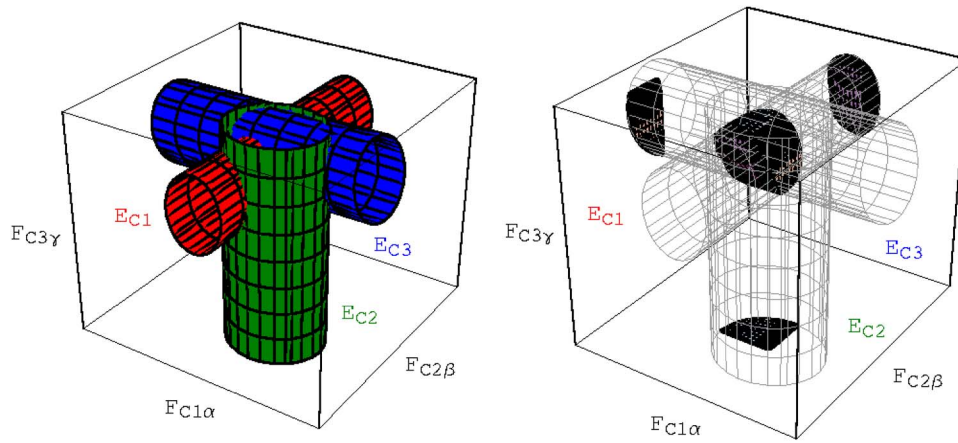
Fig. 6   The solution volume representation

opening up each friction cone with identical rates for a contact point priority ratio of 1:1:1 for contact points C_1, C_2, and C_3 ($P_{C1}:P_{C2}:P_{C3}=1:1:1$) and Fig. 5(b) shows opening up each friction cone with different rates: the friction cone at contact point C_2 is opened up three times the rate of that of contact point C_1, and two times the rate of that of contact point C_3, thus applying contact point priority ratio of 3:1:2 for contact points C_1, C_2 and C_3 ($P_{C1}:P_{C2}:P_{C3}=3:1:2$).

As the friction cones are being opened up, if one intermediate friction coefficient μ_{Ci}^{*} reaches it actual value μ_{Ci} (its maximum limit) before the others, then the intermediate friction coefficient for that particular contact point remains the same while the friction cones for the other two contact points continue to be opened up until a solution is found. If this happens, it simply indicates that that particular contact point cannot satisfy the given contact point priority requirement, but the strategy continues to search for a solution that best matches the given contact point priority requirement for the other two contact points. If a solution is found this way, the contact force at the contact point that reached its maximum friction coefficient will have a margin against slip value of zero, indicating that it is at the verge of slipping.

4.2   Checking the Existence of a Solution. To implement the strategy described above, we need a method for checking the existence of a solution for a system with a given set of friction coefficients. Mathematically this task is to verify the existence of a set of three variables (the three force component variables $F_{C1\alpha}$, $F_{C2\beta}$, $F_{C3\gamma}$) that will satisfy the set of three quadratic inequality equations with two variables each, similar to Eqs. (9)–(11). This can also be understood geometrically as checking the existence of a solution volume (Hong and Cipra [16–18]) as the intersection of the projections of the three conic sections in three-dimensional space as shown in Fig. 6. However, there seems to be no easy analytical way of doing this, and thus an incremental strategy is presented as a method for checking the existence of a solution.

To check the existence of a solution for a given system with the specified friction coefficients, first we find the initial range for a force component variable using the two conic sections that involve this force component variable. Then, starting from one side of this interval, we check if a solution exists for this value of the force component variable by computing the range of the other two force components using the two conic sections, and checking if there is a set of forces in this range that satisfies the other conic section inequality constraint. If there is no solution, we increase the force component variable by a specified amount and repeat the process until a solution is found or until the end of the range is reached. If the end of the range is reached without any solutions found, no solution exists for the given friction coefficients. This process is easier to understand if shown on the force space graph

as will be presented next using the example system.

For the example system with conic sections E_{C1}, E_{C2} and E_{C3}, let us say we want to check if a solution exists with a particular set of friction coefficients

$$\mu_{C1}^{*}=0.120, \quad \mu_{C2}^{*}=0.192, \quad \mu_{C3}^{*}=0.090 \tag{16}$$

where $\mu_{Ci}^{*}=\tan\phi_{Ci}^{*}$. With these intermediate friction coefficients, the three conic sections E_{C1}^{*}, E_{C2}^{*}, and E_{C3}^{*} are found as

$$E_{C1}^{*}(F_{C3\gamma},F_{C1\alpha})=0.412F_{C3\gamma}^{2}+0.679F_{C1\alpha}^{2}+0.003F_{C3\gamma}F_{C1\alpha}$$
$$-1.821F_{C3\gamma}-1.292F_{C1\alpha}+2.472$$
$$\leq 0 \tag{17}$$

$$E_{C2}^{*}(F_{C1\alpha},F_{C2\beta})=0.522F_{C1\alpha}^{2}+0.643F_{C2\beta}^{2}+0.081F_{C1\alpha}F_{C2\beta}$$
$$-1.705F_{C1\alpha}-1.512F_{C2\beta}+1.827$$
$$\leq 0 \tag{18}$$

$$E_{C3}^{*}(F_{C2\beta},F_{C3\gamma})=0.585F_{C2\beta}^{2}+0.577F_{C3\gamma}^{2}+0.369F_{C2\beta}F_{C3\gamma}$$
$$-3.829F_{C2\beta}-3.840F_{C3\gamma}+9.306\leq 0 \tag{19}$$

which are shown on the force space graph in Fig. 7. The superscript "*" in the notation for the friction coefficients and the conic sections shown above indicates that these values and equations are not for the original friction cones of the system, but rather for the intermediate friction cones that are being opened up corresponding to μ_{Ci}^{*}, the intermediate friction coefficient for contact point C_i.

Choosing $F_{C1\alpha}$ as the force component variable (any of the three force components $F_{C1\alpha}$, $F_{C2\beta}$, or $F_{C3\gamma}$ can be chosen) we first find the initial range for $F_{C1\alpha}$ using the two conic sections E_{C1}^{*} and E_{C2}^{*} (Eqs. (18) and (19)) which both have $F_{C1\alpha}$ as one of its variables. Graphically, this initial range is the common range between the two projections of each conic section E_{C1}^{*} and E_{C2}^{*} on the $F_{C1\alpha}$ axis as shown in Fig. 7. This interval found for $F_{C1\alpha}$ is bounded by its minimum and maximum values as $(F_{C1\alpha})_{min}^{*}\leq F_{C1\alpha}\leq(F_{C1\alpha})_{max}^{*}$, where

$$(F_{C1\alpha})_{max}^{*}=1.419, \quad (F_{C1\alpha})_{min}^{*}=0.779 \tag{20}$$

Note that if both conic sections are not ellipses, circles, or points (the case when the conic sections are one of hyperbolas, parabolas, lines, or two non-parallel lines), the projection of the conic sections can have open intervals and thus the interval of $F_{C1\alpha}$ may not be bounded on both sides. In such cases, a bound that limits the magnitude of that force must be specified.

Once the interval for $F_{C1\alpha}$ is found, we vary the value of $F_{C1\alpha}$ in this interval and check if a solution exists. Starting from one
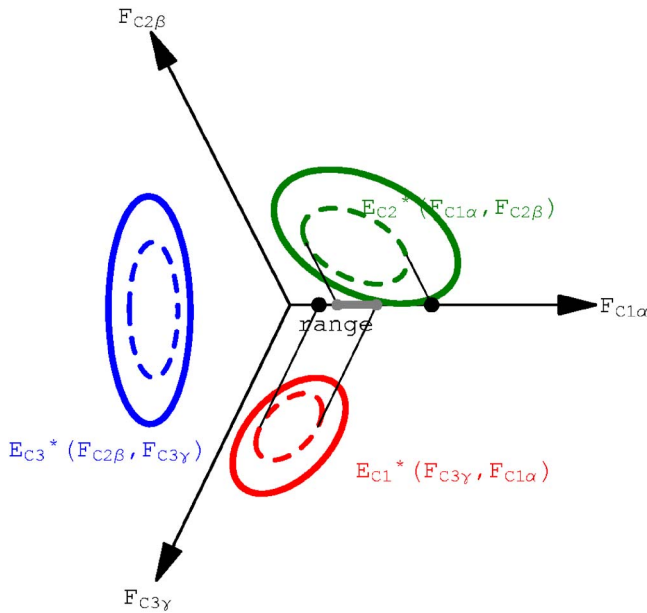
Fig. 7   Finding the initial range for $F_{C1\alpha}$ Using $\vec{E}_{C1}^*$ and $\vec{E}_{C2}^*$

side of the interval, say $(F_{C1\alpha})_{min}^*$, we check if a solution exists by computing the ranges for the other two force components $F_{C2\beta}$ and $F_{C3\gamma}$ for the current $F_{C1\alpha}$ value using Eqs. (17) and (18), and check if there is a set of values for $F_{C2\beta}$ and $F_{C3\gamma}$ in these ranges that also satisfies the E_{C3}^* conic section inequality equation (Eq. (19)).

Figure 8 shows this process of checking the existence of a solution for a value of $F_{C1\alpha}$ in its interval. The ranges for the two force components $F_{C2\beta}$ and $F_{C3\gamma}$ are represented as a parallelogram on the force space graph as shown in Fig. 8. For this particular $F_{C1\alpha}$ value, the $(F_{C2\beta}, F_{C3\gamma})$ parallelogram does not intersect with the conic section E_{C3}^*, and thus no solution exists for this $F_{C1\alpha}$ value.

This process is continued until a solution (intersection between
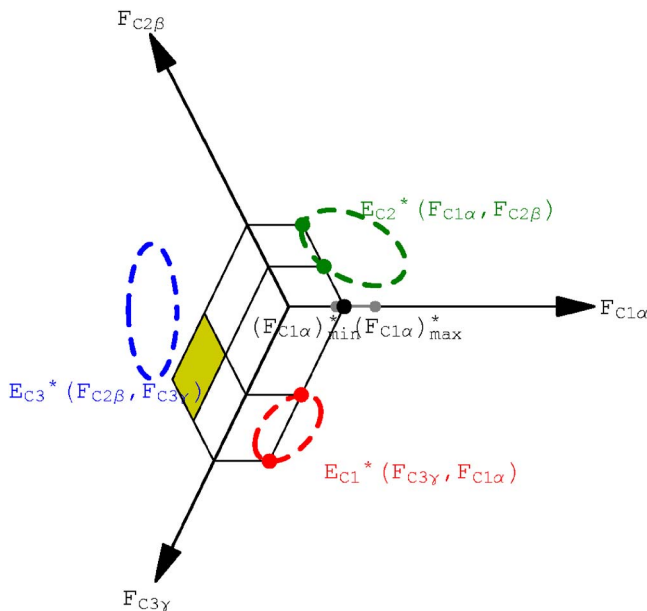
Fig. 8   The $F_{C2\beta}$, $F_{C3\gamma}$ range as a parallelogram ($F_{C1\alpha}=0.907$, no solution)
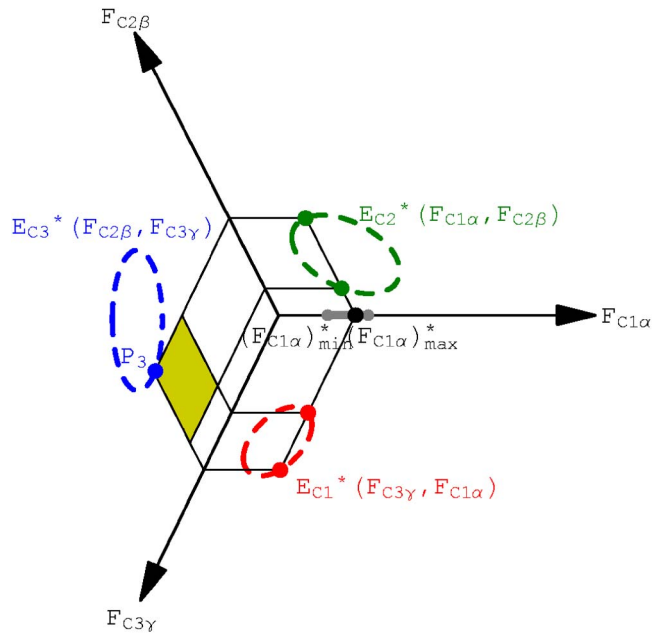
Fig. 9   The first intersection between the ($F_{C2\beta}$, $F_{C3\gamma}$) parallelogram and the conic section $\vec{E}_{C3}^*$ ($F_{C1\alpha}=1.211$)

the $(F_{C2\beta}, F_{C3\gamma})$ parallelogram and the conic section E_{C3}^*) is found, or until the end of the $F_{C1\alpha}$ interval is reached. For this example system, a solution is found before the end of the $F_{C1\alpha}$ interval is reached, and this first intersection between the parallelogram and the conic section is shown in Fig. 9. At this instant, the value for the force component variable $F_{C1\alpha}$ and the $F_{C2\beta}$, $F_{C3\gamma}$ coordinates of this first intersection point are found as

$$F_{C1\alpha} = 1.211, \quad F_{C2\beta} = 1.721, \quad F_{C3\gamma} = 2.678 \qquad (21)$$

and thus a solution exists.

4.3   Optimal Solution. The particular set of three friction coefficients used above (Eq. (16)) to illustrate the strategy for checking the existence of a solution which produced the three conic sections E_{C1}^*, E_{C2}^*, and E_{C3}^* (Eqs. (17)–(19)), is actually the set of three friction coefficients corresponding to when the first solution was found as the friction coefficients were being increased for the example system using a priority ratio of 1:1:1. Thus the $F_{C2\beta}$, $F_{C3\gamma}$ coordinates of this first intersection point together with the value of $F_{C1\alpha}$ at this instant (Eq. (21)) as shown in Fig. 9, are the only solution for this particular set of friction coefficients and thus form the three force component values for the optimal solution using the margin against slip criteria. Note that there are other solutions if the friction cones are continued to be opened, but the optimal solution set is the one that is found first which guarantees the smallest friction cone openings, thus highest margin against slip values. This set of three force components is shown on the force space graph in Fig. 10. From these three force component variables $F_{C1\alpha}$, $F_{C2\beta}$, and $F_{C3\gamma}$ that optimize the contact forces (Eq. (21)), and the three linear relationships previously found by summing the forces in the e_δ direction at the three contact points (Eqs. (6)–(8)) we can find the remaining three force components $F_{C2\alpha}$, $F_{C3\beta}$, and $F_{C1\gamma}$ as

$$F_{C2\alpha} = -1.259, \quad F_{C3\beta} = -1.688, \quad F_{C1\gamma} = -2.590 \qquad (22)$$

With the e_δ component forces previously found by summing the moments about e_α, e_β and e_γ (Eq. (5)) we have now found all force components that completely describe all contact forces that not only satisfy the static equilibrium conditions and the friction constraints, but also optimize the contact force distribution fol-
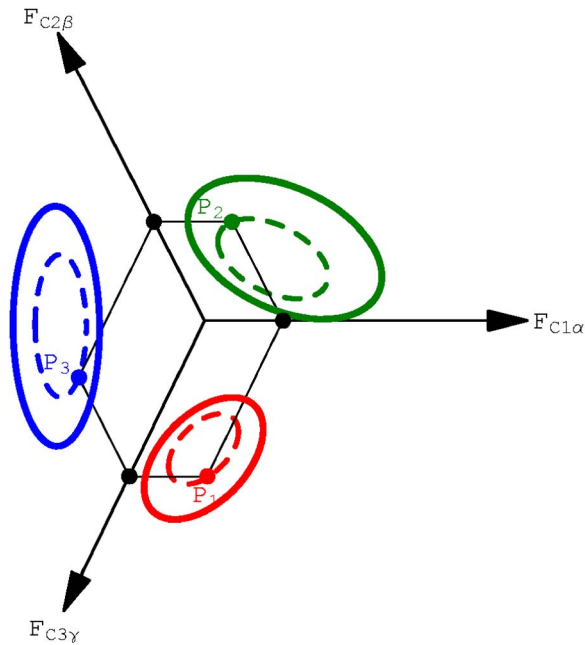
Fig. 10 Optimal solution shown in the force space graph

lowing the margin against slip criteria with contact point priority.

Expressing these foot contact forces with respect to the Cartesian X-Y-Z body coordinate frame, the final optimal force distribution is found as

$$\bar{F}_{C1} = \{-2.393, -2.336, 1.827\}$$

$$\bar{F}_{C2} = \{1.997, -1.594, 1.872\}$$

$$\bar{F}_{C3} = \{0.396, 3.830, 4.300\} \tag{23}$$

This final optimal force solution is shown to scale in Fig. 11.

The margin against slip (N_{Ci}) at each contact point for the three feet contact case is defined as one minus the ratio of ϕ_{Ci}^* to ϕ_{Ci}
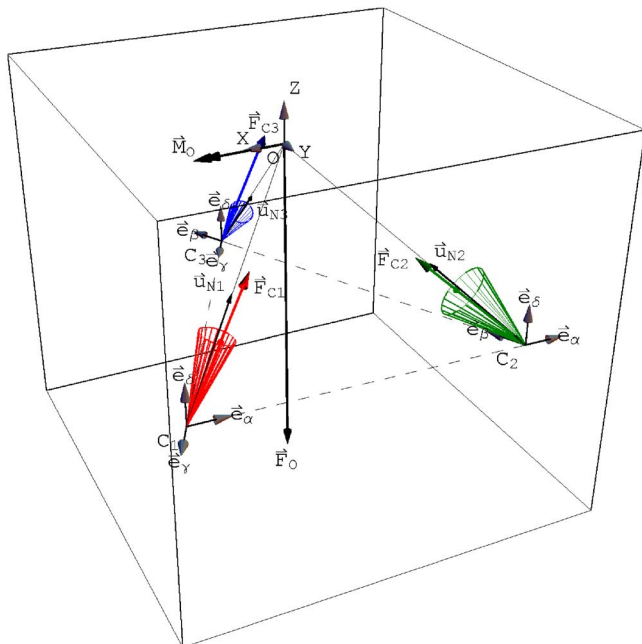
Fig. 11 The optimal solution (margin against slip criteria)

where ϕ_{Ci}^* is the friction cone angle when the first solution is found and ϕ_{Ci} is the actual friction cone angle. This can also be expressed in terms of the coefficient of friction which is the tangent of the friction cone angle, and hence

$$N_{Ci} = 1 - \frac{\phi_{Ci}^*}{\phi_{Ci}} = 1 - \frac{\tan^{-1}\mu_{Ci}^*}{\tan^{-1}\mu_{Ci}} \tag{24}$$

Using this expression, the margin against slip for each foot contact point is found as

$$N_{C1} = 0.395, \quad N_{C2} = 0.388, \quad N_{C3} = 0.397 \tag{25}$$

which are the largest possible values obtainable whose priority ratio is close to 1:1:1.

5 Other Optimization Criteria and Approaches

In this paper, we have presented the strategy for finding the optimal solution using the margin against slip with contact point priority criteria for its simplicity and usefulness. However, there can be many other possible ideas for different optimization criteria where each of them would have different uses for different situations with their own geometrical interpretations that would give other useful insights and information for the system.

One potentially useful strategy for choosing the optimal solution is to use the "solution volume" representation (Hong and Cipra[16–18]). The solution volume is defined as the volume created by the intersection of the projections of the three conic sections (E_{C1}, E_{C2}, and E_{C3}) in three-dimensional space as shown in Fig. 6. Any point defined by the three contact force components that is in this solution volume is a solution that satisfies all static equilibrium and friction constraints. One way of using the solution volume for choosing the optimal solution would be to choose the "center point" of the solution volume. This center point would then be the point furthest from the boundaries of its solution space, providing the maximum safety margin against failure in all directions. However, the location of this optimal point would depend on the definition for the center we choose to use.

One way of defining the center point for the solution volume may be to fit the maximum size sphere in the three-dimensional solution volume and to define the center to be the center point of the solution space. The size of this sphere, which is defined by its radius, can then be used as a parameter to indicate the quality of its solution space (the larger the radius the better the solution space). A new definition of a margin against slip can be used for such a case where it is defined as one minus the ratio of the distance of the chosen solution to the center point, over the radius of the sphere. Using this new definition, this factor would have a value between one and zero, where the optimal point would always have a value of one, and a solution point on the surface of the sphere would have a value of zero (even though it might not be at the verge of failure).

Another way to implement this idea may be to fit a rectangular parallelepiped volume with a certain length to height to width ratio inside the solution volume, instead of a sphere. This length to height to width "priority ratio" for this "box" may be used to implement a concept similar to the idea of contact point priority.

Instead of using a rectangular parallelepiped inside the solution volume with varying length, height, width ratios, an easier way might be to define the smallest rectangular parallelepiped box which inscribes the solution volume. This box would then have an easy to compute predetermined length, height, width ratio. The center point of this box (a point defined using the midpoint of the length, height, and width of the box) may be chosen as the optimal solution for the system. This method may computationally be the easiest and fastest way to choose a solution, however, it is not an accurate way to define the optimal solution. However, in certain situations, this strategy may still be a useful method for choosing a "good enough" solution quickly.

6 Summary and Conclusion

In this paper, we have presented a method for choosing the optimal force distribution solution in the solution space for the three feet contact case. Using the 'force space graph' representation scheme as a tool, the optimal solution is chosen by selecting the values for the three parameters that define the solution. The margin against slip criteria with contact point priority was presented and a strategy of opening up the friction cones while checking the existence of a solution was developed to implement the choosing of the optimal solution. Discussions of the geometric interpretation of the procedure and results were presented using an example to provide insight into the complex interaction of the contact force components and to visually give insight into the physical meanings of the parameters involved. Other ideas for optimization criteria based on the solution volume representation were discussed. Future research areas may include developing other concepts for the optimization criteria and developing strategies to implement them in choosing the optimal solution.

References

[1] Klein, C. A., and Chung, T., 1987, "Force Interaction and Allocation for the Legs of a Walking Vehicle," IEEE J. Rob. Autom., **3**(6), pp. 546–555.
[2] Klein, C., Olson, K., and Pugh, D., 1983, "Use of Force and Attitude Sensors for Locomotion of a Legged Vehicle Over Irregular Terrain," Int. J. Robot. Res., **2**(2), pp. 3–7.
[3] Salisbury, J. K., and Craig, J. J., 1982, "Articulated Hands: Force Control and Kinematic Issues," Int. J. Robot. Res. **1**(1), pp. 4–17.
[4] Kumar, V. R., and Waldron, K. J., 1988, "Force Distribution in Closed Kinematic Chains," IEEE J. Rob. Autom., **4**(6), pp. 657–664.
[5] Zuo, B., and Qian, W., 1999, "On the Equivalence of Internal and Interaction Forces in Multifingered Grasping," IEEE Trans. Rob. Autom., **15**(5), pp. 934–941.
[6] Yoshikawa, T., and Nagai, K., 1991, "Manipulating and Grasping Forces in Manipulation by Multifingeres Robot Hands," IEEE Trans. Rob. Autom., **7**(1), pp. 67–77.
[7] Klein, C. A., and Kittivatcharapong, S., 1990, "Optimal Force Distribution for the Legs of a Walking Machine With Friction Cone Constraints," IEEE Trans. Rob. Autom., **6**(1), pp. 73–85.
[8] Nahon, M. A., and Angeles, J., 1992, "Real-Time Force Optimization in Parallel Kinematic Chains Under Inequality Constraints," IEEE Trans. Rob. Autom., **8**(4), pp. 439–450.
[9] Chen, X., Watanabe, K., Kiguchi, K., and Izumi, K., 1999, "Optimal Force Distribution for the Legs of a Quadruped Robot," Mach. Intell. Rob. Control, **1**(2), pp. 87–94.
[10] Cheng, F., Chen, T., and Sun, Y., 1994, "Resolving Manipulator Redundancy Under Inequality Constraints," IEEE Trans. Rob. Autom., **10**(1), pp. 65–71.
[11] Chen, J., Cheng, F., Yang, K., Kung, F., and Sun, Y., 1999, "Optimal Force Distribution in Multilegged Vehicles," Robotica, **17**(2), pp. 159–172.
[12] Kerr, J. R., and Roth, B., 1986, "Analysis of Multifingered Hands," Int. J. Robot. Res., **4**(4), pp. 3–17.
[13] Kumar, V., and Waldron, K. J., 1989, "Suboptimal Algorithms for Force Distribution in Multifingered Grippers," IEEE Trans. Rob. Autom., **5**(4), pp. 491–498.
[14] Cheng, F., and Orin, D. E., 1990, "Efficient Algorithm for Optimal Force Distribution—The Compact Dual LP Method," IEEE Trans. Rob. Autom., **6**(2), pp. 178–187.
[15] Hong, D. W., and Cipra, R. J., 2002, "Optimal Force Distribution for Tethered Climbing Robots in Unstructured Environments," *Proceedings of the ASME 2002 Design Engineering Technical Conferences and Computers and Information in Engineering Conference, Montreal*, Canada, September 29-October 2.
[16] Hong, D. W., 2002, "Analysis and Visualization of the Contact Force Solution Space for Multi-Limbed Mobile Robots," Ph.D. dissertation, Purdue University, West Lafayette, IN.
[17] Hong, D. W., and Cipra, R. J., 2003, "Analysis and Visualization of the Contact Force Solution Space for Multi-Limbed Mobile Robots with Three Feet Contact," *Proceedings of the ASME 2003 DETC*, Chicago, September 2–6.
[18] Hong, D. W., and Cipra, R. J., 2006, "Visualization of the Contact Force Solution Space for Multi-Limbed Robots," ASME J. Mech. Des., **128**(1), pp. 295–302.
[19] Mason, M. T., and Salisbury, J. K., 1985, "Robot Hands and the Mechanics of Manipulation," MIT Press, Cambridge, MA.
[20] Ghafoor, A., Dai, J. S., and Duffy, J., 2004, "Stiffness Modeling of the Soft-Finger Contact in Robotic Grasping," ASME J. Mech. Des., **126**(4), pp. 646–656.